Albedo Solution to Global Warming

In the Control of CO_2, Hotspots, & Hydro-Hotspots Forcing and Their Albedo-GHG Interactions

Alec Feinberg
DfRSoft Research, email: dfrsoft@gmail.com

Key Words: Albedo Solution, Reflectivity Solution, Hotspot Forcing, Hydro-Hotspots Forcing, Re-Radiation Model, Albedo-GHG Interaction

Abstract

Due to the slow progress being made in climate change mitigation and the threat of tipping points, albedo solutions could be a vital supplement to CO_2 reduction efforts. An important aspect to bring to the attention of policymakers is the albedo-greenhouse gas (GHG) interaction strength. We model this interaction which has a major influence in assessing climate change. For example, modeling is used to help exemplify the amount of reverse forcing or albedo surface area modification required to mitigate CO_2 GW effects. Additionally, albedo controls are the only way to mitigate impermeable hotspots and hydro-hotspots surfaces that have increased at an alarming rate. We illustrate their growth rate; discuss their historical recognized significance and known correlations to climate change. Our results are directed toward influencing policymakers on the unique practical aspects of albedo solutions and their imminent need.

1. Introduction

Although albedo solutions have been recommended in helping to mitigate climate change [1-12] as a highly important supplement to CO_2 efforts, little work is being done in this area. There have been a number of proposed albedo solutions, both surface and atmospheric methods [1, 4-10] to reduce climate change. Such techniques have not been widely adopted by governments [9] and were not part of the Paris Climate Accord [13].

In this paper, we describe the albedo-GHG interactions that applies to three observed forcing issues and using historical information, model its strength and discuss its unique role for potential albedo solutions in climate controls. This provides guidance to policymakers on the increase strength of albedo solutions that are optimum as the only controls in mitigating all three types of forcing. Thus, this interaction strength is important for both solar surface and atmospheric geoengineering in assessing such climate controls and directing climate policy. Modeling has shown [11] that the cumulative effect of widespread select albedo-GHG mitigation of surface areas, can have significant influence both to the Earth's solar surface heat absorption and associated GHG re-radiation power. Therefore, albedo solutions could prove to be vital in helping prevent a 1.5°C-3°C rise and consequently stopping tipping points [1-8] from occurring. We are hopeful this work will help contribute to influencing climate policy and related funding.

2. Method

It is helpful to describe the albedo-GHG interactions and associated historical information for three types of observed GW forcing issues:

- CO_2 (ignoring other GHGs)
- Hotspots (such as Urban Heat Islands (UHIs) and Roads)
- Hydro-hotspots

We term a hydro-hotspot [14] as a solar hot impermeable surface common in cities and roads that creates atmospheric moisture in the presence of precipitation. This moisture increase can act as a local greenhouse gas. A possible mechanism includes warmer expanded air-surface temperatures due to the initial hotspot, and then during precipitation, evaporation increases the local atmosphere humidity GHG (as warm air holds more water vapor). The level of hydro-hotspot significance in climate change is currently unknown.

However observations of this effect are reasonably well established. For example, Zhao et al. [15] observed that UHI temperatures increase in daytime ΔT by 3.0^{o}C in humid climates but decrease ΔT by 1.5^{o}C in dry climates. They found a strong correlation between ΔT increase and daytime precipitation. Their results concluded that albedo management would be a viable means of reducing ΔT on large scales.

A major benefit of the albedo solution often overlooked is the interaction strength with the greenhouse gas mechanism which arises from the simple fact that

- *Increasing the reflectivity of a hotspot surface reduces its greenhouse gas effect*
- *Decreasing the reflectivity of a hotspot surface increases its greenhouse gas effect*
- *The Global Warming (GW) change associated with a reflectivity hotspot modification is given by the albedo-GHG radiation factor having an approximate inherent value of 1.6 (Sec. 2.2).*

Therefore, albedo solutions [1-12] are proficient, ***and the only climate control having strong distinct mitigation interactions with all three forcing mechanisms***. This simple knowledge could be helpful in educating policymakers on realizing the value of the albedo solution.

- In Section 2.2, we detail this 1.6 average albedo-GHG interaction strength for solar geoengineering and provide estimates of this additional GHG effect in two different time periods, 1950 and 2019.
- In Section 4, we specifically show how practical the albedo solutions are for reverse forcing increases caused by CO_2 levels (see also Eq. 23).

It is important to note that the albedo-GHG heat exchange is often dominated with water vapor and clouds GHG, 36-72% compared with CO_2 GHG 9-26% [16]. This provides a possible breakdown of the GHG power, but not the forcing strengths [17, 18]. Due to this interaction, albedo solutions would decrease risks of GHG effects, hydro-hotspot forcing as well as the possible significance of hotspots. Since hydro-hotspots create higher warming impact in humid climates, these select widespread urban surface areas generally have higher GW impact and mitigating albedo surface solutions in these regions would be desirable.

The significance of hotspot forcing has been highly controversial in global warming as it relates to UHIs. Measurements and their assessments have been described by a number of authors [19-29] and more recently in modeling [11, 30]. One key work often referred to is by McKitrick and Michaels [19, 20] that concluded about half the reported warming trend in global-average land surface air temperature in 1980–2002 resulted from local land-surface changes (i.e. urbanization and other manmade surface changes).
.
Although this study has been severely criticized especially by Schmidt [31] and defended successfully by Mckitrick [20] over many years, the research still remains apparently difficult to accept. Nevertheless, these results [19-29], completed over 10 years ago, have not been influential for implementing worldwide albedo controls and solutions [32]. For example, such solutions were not part of the Paris Climate Accord [13].

In modeling recently, by the author [11, 30], UHI amplification factors were estimated (for solar area, heat capacity, surface albedo, canyon effect, etc.) with the help of UHI footprint and dome estimates that extended

the UHI effect beyond its own area and applied to albedo modeling. Appendix A provides an overview of these factors. Results showed feasible support for these authors' findings [19-29] that UHIs can significantly contribute to GW with one model showing 4.5%-38% [30] and a second model showing 6%-82% [11] of GW could be due to UHIs. These large variations are due to uncertainties in UHI amplification factors and estimates of how much of the Earth is urbanized.

Given the controversies and current need, now is a good time to add measures and working groups to find alternate supplemental feasible albedo solutions. Whether or not hotspots are a significant source in climate change is independent of the fact that surface and atmospheric albedo controls can provide strong aid in reducing climate change [1-12] and the practicality of surface solutions has been demonstrated by the author [11] (see also Sec. 4). Therefore, implementation of surface and/or atmospheric albedo controls and methods should be an added focus in obtaining appropriate policy.

- ***Policymakers can recommend surface and atmospheric albedo controls conservatively in the event that hotspots and hydro-hotspots are reasonably significant and also to offset CO_2 GW effects through enhanced albedo solutions (See Sec. 4 for a CO_2 albedo mitigation example)***

Little is understood about related hydro-hotspot GW forcing significance. However, since the industrial revolution, impermeable surfaces have increased at a high rate (like CO_2) correlated to population growth and thus, GW increases [30]. This is illustrated in Figure 1 that shows correlations to both GW and population growth to natural aggregates that are used to build cities and roads. Although no definitive conclusion can be made on GW significance, it is important to point out the growth rate of impermeable surfaces, as they have a high level of concern with numerous issues related to climate change [33-39].

- ***Policymakers should recommend world-wide surface albedo hotspot controls in the construction of UHIs, rooftops, roads, parking lots, car colors, and so forth. Working groups are needed to provide optimum solutions [1-11].***

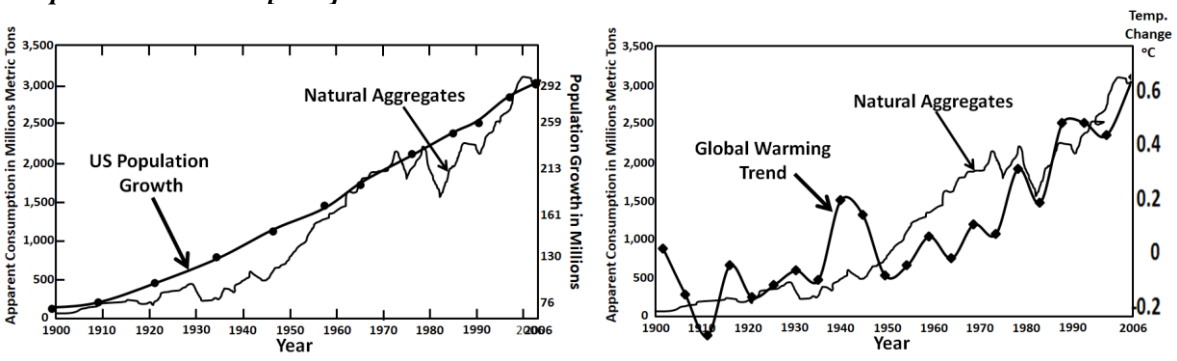

Figure 1 a) Natural aggregates [40] correlated to U.S. Population Growth (USGS [41]) **b)** Natural aggregates [40] correlated to global warming (NASA [42])

In terms of amplification effects, hydro-hotspots would likely have both local water-vapor GHG interactions and the additional 1.6 warming influence on GW (with UHI heat capacity also playing an important role).

Lastly, one can justify the need for albedo controls due to the:

- slow progress reported in CO_2 reduction
- yearly increases in reports on large desertification and deforestation occurring [43]
- lack of hotspot and hydro-hotspot surface albedo controls that are continually increasing
- threat of the tipping point occurring as we are running out of time

Regarding the interactive strength, it is helpful to determine the geoengineering albedo-GHG re-radiation 1.6 factor [11] and its change since the pre-industrial revolution. Such values relate to the effective emissivity constant of the planetary system. Results will also help to demonstrate how albedo solution can offset CO_2 forcing (see Sec. 4) for policymakers. Therefore, assessment helps to strengthen interests in albedo solutions.

2.1 Albedo-GHG Radiation Factor

In geoengineering the albedo-GHG interaction requires a different approach compared to CO_2 doubling theory. When initial solar absorption occurs, part of the long wavelength radiation given off is re-radiated back to Earth. In the absence of forcing we denote this fraction as f_1. This presents a simplistic but effective model

$$P_{\mathrm{Pre-Industrial}} = P_\alpha + P_{GHG} = P_\alpha + f_1 P_\alpha = P_\alpha \left(1 + f_1\right) = \sigma T_S^4 \text{ where } P_\alpha = \frac{S_o}{4}(1-\alpha) \tag{1}$$

and T_s is the surface temperature, $P_{\text{pre-industrial}}$, P_α, and P_{GHG} are the total pre-industrial warming, albedo warming and GHG warming in W/m^2, respectively. As one might suspect, f_1 turns out to be exactly β^4 in the absence of forcing, so that f_1 is a redefined variable taken from the effective emissivity constant of the planetary system. We identify $1+f_1=1.618034$ (see Section 2.2) as the pre-industrial albedo-GHG radiation factor (Table 1).

We identify the re-radiation 2019 having a value of $1+f_2=1.6276$ (Table 1). That is, in 2019, due to increases in GHGs, an increase in the re-radiation fraction occurs

$$f_2 = f_{2019} = f_1 + \Delta f = \beta_1^4 + \Delta f \approx \beta_2^4 + \Delta f \tag{2}$$

In this way $f_{2019} = f_2$ is a function of f_1. The RHS of Eq. 2 indicates that $\beta_1 \approx \beta_2$ (see verification results in Eq. 18 and 19). We find that $\Delta f=0.0096$ is relatively small compared to $(1+f_1)$ which we show can fairly accurately be assessed in geoengineering.

2.2 Estimating the Pre-industrial Albedo-GHG Interaction Strength

In geoengineering, we are working with absorption and re-radiation, we define

$$P_{Total} = \sigma T_S^4 = \sigma\left(\frac{T_e}{\beta}\right)^4 \text{ and } P_\alpha = \sigma T_\alpha^4 = \sigma\left(\beta T_S\right)^4 \tag{3}$$

The definitions of $T_\alpha=T_e$, T_S and β are the emission temperature, surface temperature and typically $\beta \approx 0.887$, respectively. Consider a time when there is ***no forcing issues*** causing warming trends. Then by conservation of energy, the equivalent power re-radiated from GHGs in this model is dependent on P_α with

$$P_{GHG} = P_{Total} - P_\alpha = \sigma T_S^4 - \sigma T_\alpha^4 \tag{4}$$

To be consistent with $T_\alpha=T_e$, since typically $T_\alpha \approx 255^oK$ and $T_s \approx 288^oK$, then in keeping with a common definition of the global beta (the proportionality between surface temperature and emission temperature) for the moment $\beta=T_\alpha/T_s=T_e/T_S$.

This allows us to write the dependence

$$P_{GHG} = \sigma T_S^4 - \sigma T_\alpha^4 = \frac{\sigma T_\alpha^4}{\beta^4} - \sigma T_\alpha^4 = \sigma T_\alpha^4\left(\frac{1}{\beta^4} - 1\right) = \sigma T_\alpha^4\left(\frac{1}{f} - 1\right) \tag{5}$$

Note that when $\beta^4=1$, there are no GHG contributions. We note that f, the re-radiation parameter equals β^4 in the absence of forcing.

We can also define the blackbody re-radiated by GHGs given by some fraction f_1 such that

$$P_{GHG} = f_1 P_\alpha = f_1 \sigma T_\alpha^4 \tag{6}$$

Consider f=f_1, in this case according to Equations 5 and 6, it requires

$$P_{GHG} = \sigma T_\alpha^4 \left(\frac{1}{f_1} - 1 \right) = f_1 \sigma T_\alpha^4 \tag{7}$$

This dependence leads us to the solution of the quadratic expression

$$f_1^2 + f_1 - 1 = 0 \text{ yielding } f_1 = 0.618034 = \beta^4,\ \beta = \left(0.618034\right)^{1/4} = 0.886652 \tag{8}$$

This is very close to the common value estimated for β and this has been obtained through energy balance in the planetary system providing a self-determining assessment. In geoengineering we can view the re-radiation as part of the albedo effect. Consistency with the Planck parameter is shown in Section 3.1. We note that the assumption f=f_1 only works if planetary energy is in balance without forcing. In the next section, we double check this model in another way by balancing energy in and out of our global system.

2.3 Balancing Pout and Pin in 1950

In equilibrium the radiation that leaves must balance P_α, the energy absorbed, so that

$$\begin{aligned} Energy_{Out} &= (1-f_1)P_\alpha + (1-f_1)P_{Total} = (1-f_1)P_\alpha + (1-f_1)\left\{P_\alpha + f_1 P_\alpha\right\} \\ &= 2P_\alpha - f_1 P_\alpha - f_1^2 P_\alpha = Energy_{In} = P_\alpha \end{aligned} \tag{9}$$

This is consistent, so that in 1950, Eq. 9 requires the same quadratic solution as Eq. 8. It is also apparent that

$$P_\alpha = f_1 P_{Total\_1950} = \beta_1^4 P_{Total\_1950} \tag{10}$$

since

$$P_\alpha = f_1(P_\alpha + f_1 P_\alpha) \ \ or \ \ 1 = f_1(1+f_1) \tag{11}$$

The RHS of Eq. 11 is Eq. 8. This illustrates f_1 from another perspective as the fractional amount of total radiation in equilibrium. As a final check, the application in the Section 3, in Table 1, illustrates that f_1 provides reasonable results.

2.4 Re-radiation Model Applied to 2019

In 2019 due to global warming trends, to apply the model we assume that feedback can be applied as a separate term and we make use of some IPCC estimates for GHG forcing as a way to calibrate our model. In the traditional sense of forcing, we assume some small change to the albedo and most of the forcing due to IPCC/NOAA estimates for GHGs where

$$P_{Total\,2019} = P_{\alpha'} + P_{GHG'} = P_{\alpha'}(1+f_2) \tag{12}$$

Then we introduce feedback through an amplification factor A_F as follows

$$P_{Total\,2019\,\&\,Feedback} = P_{1950} + \left(\Delta P\right) A_F = P_{1950} + \left(P_{2019} - P_{1950}\right) A_F = \sigma T_S^4 \tag{13}$$

Here, we assume a small change in the albedo denoted as P_α' and f_2 is adjusted to the IPCC GHG forcing value estimated between 1950 and 2019 of 2.38W/m^2 [18]. Although this value does not include hydro-hotspot forcing assessment described in the introduction, it possibly may be effectively included since forcing

estimates also relate to accurate GW temperature changes. Then the feedback amplification factor, is calibrated so that T_S=T_{2019} (see Table 1) yielding A_F =2.022 [also see ref. 44]. The main difference in our model is that the forcing is about 6% higher than the IPCC for this period. Here, we take into account a small albedo decline of 0.15% that the author has estimated in another study due to likely issues from UHIs [30] and their coverage. We note that unlike f_1, f_2 is not a strict measure of the emissivity due to the increase in GHGs.

3. Results Applied to 1950 and 2019 with an Estimate for f_2

In 1950 we will simplify estimates by assuming the re-radiation parameter is fixed and reasonable close to the pre-industrial level of f_1=0.618034. Then, to obtain the average surface temperature T_{1950}=13.89°C (287.04°K), the only adjustable parameter left in our basic model is the global albedo (see also Eq. 1). This requires an albedo value of 0.3008 (see Table 1) to obtain the T_{1950}.=287.04°K. This albedo number is reasonable and similar to values cited in the literature [45].

In 2019, the average temperature of the Earth is T_{2019}=14.84°C (287.99°K) given in Eq. 15. We have assumed a small change in the Earth's albedo due to UHIs [30]. The f_2 parameter is adjusted to 0.6276 to obtain the GHG forcing shown in Column 7 of 2.38W/m^2 [18]. Therefore the next to last row in Table 1 is a summary without feedback, and the last row incorporates the A_F=2.022 feedback amplification factor.

Table 1 Model Results

Year	T_S(°K)	T_α(°K)	f_1, f_2	α, α'	Power Absorbed W/m^2	$P_{GHG'}$ P_{GHG}	P_{Total} W/m^2
2019	287.5107	254.55	0.6276	30.03488	238.056	149.4041	387.4605
1950	287.04	254.51	0.6180	30.08	237.9028	147.024	384.9267
Δ2019-1950	0.471	0.041	0.0096	(0.15%)	0.15352	2.38	2.53
$\Delta_{Feedback}$ A_F=2.022	0.95	0.083	-	-	0.3104	4.81	5.12

From Table 1 we now have identified the reverse forcing at the surface needed since

$$P_{Total\,2019\_Feedback\,Amp} = P_{1950} + \left(P_{2019} - P_{1950}\right) A_F = 384.927 W/m^2 + (2.5337 W/m^2)2.022 = 390.05 W/m^2 \quad (14)$$

and

$$\Delta T_S = T_{2019} - T_{1950} = \left(390.05/\sigma\right)^{1/4} - 287.04°K = 287.9899°K - 287.04°K = 0.95°K \quad (15)$$

as modeled. We also note an estimate has now been obtained in Table 1 for f_2=0.6276, A_F=2.022, and $\Delta P_{Total\_Feedback\_amp}$=5.12W/m^2.

3.1 Model Consistency with the Planck Parameter

As a measure of model consistency, the forcing change with feedback, and resulting temperatures T_{1950} and T_{2019}, should be in agreement with expected results using the Planck feedback parameter. From the definition of the Planck parameter λ_o and results in Table 1, we estimate [46]

$$\lambda_o = -4\frac{\Delta R_{OLW}}{T_S} = -4\left(\frac{237.9028 W/m^2}{287.041°K}\right)_{1950} = -3.31524 W/m^2/°K \quad (16)$$

and

$$\lambda_o = -4\frac{\Delta R_{OLW}}{T_S} = -4\left(\frac{238.056 W/m^2}{287.99°K}\right)_{2019} = -3.306 W/m^2/°K \quad (17)$$

Here ΔR_{OLW} is the outgoing long wave radiation change. We note these are very close in value showing miner error and consistency with Planck parameter value, often taken as 3.3W/m^2/^{o}K.

Also note the Betas are very consistent with Eq. 8 for the two different time periods since from Table 1

$$\beta_{1950} = \frac{T_\alpha}{T_S} = \frac{T_e}{T_S} = \frac{254.51}{287.041} = 0.88667 \; and \; \beta_{1950}^4 = 0.6180785 \tag{18}$$

and

$$\beta_{2019} = \frac{T_\alpha}{T_S} = \frac{T_e}{T_S} = \frac{254.55}{287.5107} = 0.88526 \; and \; \beta_{2019}^4 = 0.6144 \tag{19}$$

3.2 Hotspot Versus GHG Forcing Equivalency

From Equation 1 and 12 we can estimate the effect in a change in hotspot forcing as

$$\left(\frac{dP_{Total}}{dP_\alpha}\right)_{1950} = (1+f_1) = 1.618 \;\; \text{and} \;\; \left(\frac{dP_{Total}}{dP_\alpha}\right)_{2019} = (1+f_2) = 1.6276 \tag{20}$$

However, we note a change in GHGs is only a factor of 1 by comparison

$$\frac{dP_{Total}}{dP_{GHG}} = \frac{d\left(P_\alpha + P_{GHG}\right)}{dP_{GHG}} = 1 \tag{21}$$

or from Table 1 data

$$\frac{dP_{Total}}{dP_{GHG}} = \frac{2.53}{2.38} = 1.063 \tag{22}$$

This indicates 1 W/m^2 of albedo forcing generally requires 1.6 W/m^2 of GHG forcing to have the same global warming effect. Alternately, form Eq. 22 and Table 1 data this is about 1.53. This result should be helpful in albedo forcing estimates.

4. Discussion

From Table 1 we used two key forcing changes that are responsible for climate change since 1950

- Δf and $\Delta\alpha$

We know that $\Delta\alpha$ can only be mitigated by albedo controls. In Table 1, the albedo effect used was fairly minimal, contributing only a 0.15 W/m^2 (6%) to the warming. However, if we were to implement a worldwide albedo surface solution of select areas, for example, Table 2 lists the albedo amplification factors that can potentially be realized.

Table 2 Albedo Surface Solution Factors

Amplification Type	Factor
Albedo enhancement	4
Reduction of heat storage targets (Appendix A)	6
Re-radiation reduction	1.6
Total Product	**38**

Here, selecting surfaces with high heat storage capacity, such as buildings (or possibly mountains) are likely good strategic targets. These areas are a function of heat capacity, surface albedo, mass, temperature storage, solar irradiance and humid environments, which can yield amplification factors between 3.1-8.4 (averaging 6) [11, 30]. These factors are described in Appendix A to aid the reader. These estimates are not unreasonable for UHIs [11]. As well there are atmospheric albedo solutions [1-6].

Consider how this applies to Table 1 GHGs. In Table 1, Δf is controlled by GHGs assumed to be dominated by CO_2 forcing (recall that part of this may actually intrinsically include hydro-hotspots which are mitigated only by albedo methods). The reverse forcing albedo reduction to mitigate Δf when considering these albedo amplification factors applied to Table 2 is

$$\text{Reverse Forcing Mitigation Requirement} = 2.38 \text{ W/m}^2/38 = 0.063 \text{ W/m}^2 \quad (23)$$

This is a helpful results indicating less reverse forcing than one might expect. Carrying this a step further, the amount of Earth this translates to needing with reflectivity modification with albedo increase between 4-7.5 has been assessed by the author [11] for this particular problem, yielding an area of about 0.2% to 1% of the Earth, depending on the selected target types.

Therefore, we note by employing albedo solutions, reverse cooling results would help compensate for CO_2 forcing, and conservatively include hotspots and hydro-hotspots mitigation. In the event that hotspots and their associated hydro-hotspots are significant as suggested by many authors [11, 15, 19-30], this would be the optimum approach. This helps in clarifying the benefit and need for including albedo controls and solutions in climate change policies.

5. Summary

In this paper we have focused on the albedo-GHG interaction to show how the albedo solution, could be a vital method to help mitigate global warming when three types of forcing issues are considered. Such implementation would greatly supplement CO_2 solutions. Results can improve the speed in helping to prevent a tipping point from occurring (especially with desertification and deforestation occurring). Furthermore, analysis showed that the surface albedo solution can effectively compensate for CO_2 forcing without having to modify an unreasonable area of the Earth. As well, atmospheric albedo solutions are available.

The GHG-albedo interaction strength due to the re-radiation factor has been fully described in application to two time periods. Results show that the re-radiation factor for 1950 when taken as a pre-industrial value is 1.6181 which is directly given by β^4 (the emissivity constant of the planetary system). However in present day, this factor has increase to 1.6276 due to the increase in GHGs. In order to make the present day assessment, we assumed a small planetary albedo decrease from 1950 of 0.15% and GHG forcing of about 2.38 W/m^2 (in accordance with IPCC estimates). In terms of geoengineering albedo modification estimates, the interactive value of 1.62 should to be a good approximation.

Below we provide suggestions and corrective actions for policymakers to consider:

- Modification of the Paris Climate Agreement to include albedo controls and solutions
- Albedo guidelines for both UHIs and roads similar to on-going CO_2 efforts

- Guidelines for future albedo design considerations of cities
- Government money allocation for geoengineering and implement albedo solutions
- Recommend an agency like NASA to be tasked with finding applicable albedo solutions and implementing them
- Recommendation for cars to be more reflective. Although world-wide vehicles likely do not embody much of the Earth's area, recommending that all new manufactured cars be higher in reflectivity (e.g., silver or white) would help raise awareness of this issue similar to electric automobiles that help improve CO_2 emissions.

Disclosures
Funding: This study was unfunded.
Conflicts of Interest: The author declares that there are no conflicts of interest.

Appendix A: UHI Amplification Factors

An analysis of UHI amplification effects was originally provided by the author [30] and this work is added here to aid the reader.

A.1 UHI Area Amplification Factor

To estimate UHI amplification effects, it is logical to first look at UHI footprint (FP) studies as they provide some measurement information. Zhang et al. [47] found the ecological FP of urban land cover extends beyond the perimeter of urban areas, and the FP of urban climates on vegetation phenology was 2.4 times the size of the actual urban land cover. A more recent study by Zhou et al. [48], looked at day-night cycles using temperature difference measurements in China. This study found UHI effect decayed exponentially toward rural areas for the majority of the 32 Chinese cities. Their comprehensive study spanned from 2003 to 2012. Zhou et al. describes China as an ideal area to study as it has experienced the most rapid urbanization in the world during the decade evaluated. Findings state that the FP of UHI effect, including urban areas, was 2.3 and 3.9 times that of urban size for the day and nights, respectively. We note that the average day-night amplification footprint coverage factor is 3.1.

The UHI Amplification Factor (AF) is highly complex, making it difficult to assess from first principles as it would be some function of

$$AF_{UHI\ for\ 2019} = f\left(\overline{Build}_{Area}\ x\ \overline{Build}_{C_p}\ x\ \overline{R}_{wind}\ x\ \overline{LossE}_{vtr}\ x\ \overline{Hy}\ x\ \overline{S}_{canyon}\right) \tag{A-1}$$

were

$\overline{Build}_{Area}$ =Average building solar area
$\overline{Build}_{C_p}$ = Average building heat capacity
$\overline{R}_{wind}$ = Average city wind resistance
$\overline{LossE}_{vtr}$ = Average loss of evapotranspiration to natural cooling & loss of wetland
$\overline{Hy}$ = Average humidity effect due to hydro-hotspot
$\overline{S}_{canyon}$ = Average solar canyon effect

To provide some estimate of this factor, we note that Zhou et al. [48] found the FP physical area (km^2), correlated tightly and positively with actual urban size having a correlation coefficients higher than 79%. This correlation can be used to provide an initial estimate of this complex factor. Therefore, as a model assumption, it seems reasonable to use area ratios for this estimate.

$$AF_{UHI\ for\ 2019} = \frac{\sum(UHI\ Area)_{2019}}{\sum(UHI\ Area)_{1950}} \tag{A-2}$$

Area estimates have been obtained in the Feinberg [30] yielding the following results for the Schneider et al. [49] and the GRUMP [50] extrapolated area results:

$$AF_{UHI\ for\ 2019} = \frac{(Urban\ Size)_{2019}}{(Urban\ Size)_{1950}} \approx \begin{cases} \left(\frac{[0.188]_{2019}}{[0.059]_{1950}}\right)_{\text{Schneider}} = 3.19 \\ \left(\frac{[0.952]_{2019}}{[0.316]_{1950}}\right)_{GRUMP} = 3.0 \end{cases} \quad \text{(A-3)}$$

Between the two studies, the UHI area amplification factor average is 3.1. Coincidently, this factor is the same observed in the Zhou et al. [48] study for the average footprint. This factor may seem high. However, it is likely conservative as other effects would be difficult to assess: increases in global drought due to loss of wet-lands, deforestation effects due to urbanization, and drought related fires. It could also be important to factor in changes of other impermeable surfaces since 1950, such as highways, parking lots, event centers that trap heat, and so forth.

The area amplification value of 3.1 is then considered as one of our model assumptions.

A.2 Alternate Method Using the UHI's Dome Extent

An alternate approach to check the estimate of Equation A-3, is to look at the UHI's dome extent. Fan et al. [51] using an energy balance model to obtain the maximum horizontal extent of a UHI heat dome in numerous urban areas found the nighttime extent of 1.5 to 3.5 times the diameter of the city's urban area (2.5 average) and the daytime value of 2.0 to 3.3 (2.65 average).

Applying this energy method (instead of the area ratio factor in Eq. A-3), yields a diameter in 2019 compared to that of 1950 with an increase of 1.8. This method implies a factor of 2.5 x 1.8=4.5 higher in the night and 2.65 x 1.8=4.8 in the day in 1950 with an average 4.65. This increase occurs 62.5% of the time according to Fan et al., where their steady state occurred about 4 hours after sunrise and 5 hours after sunset yielding an effective UHI amplification factor of 2.9. We note this amplification factor is in good agreement with Equation A-3. Fan et al. [51] assessed the heat flux over the urban area extent to its neighboring rural area where the air is transported from the urban heat dome flow. Therefore the heat dome extends in a similar manner as observed in the footprint studies. If we use the dome concept, we obtain some vertical extent which is a logical when considering GW. We can make an assumption that the actual surface area for the heat flux is increased by the surface area of the dome. We actually do not know the true diameter of the dome, but it is larger than the assessment by Fan et al. Using the dome extend due to Fan et al. [51] applied to the area of diameter D, the amplification factor should be correlated to the ratios of the dome surface areas:

$$AF_{UHI\ for\ 2019} = \left(\frac{D_{2019}}{D_{1950}}\right)^2 = 2.9^2 = 8.4 \quad \text{(A-4)}$$

Thus, this equation is a second value. It is reasonable to use the ratios of the dome's surface area for an alternate approach in estimating the effective UHI amplification factor [30]. This provides two values, 3.1 and 8.4 to work with for upper and lower bounds averaging approximately 5.8.

References

1. Dunne D, (2018) Six ideas to limit global warming with solar geoengineering, CarbonBrief, https://www.carbonbrief.org/explainer-six-ideas-to-limit-global-warming-with-solar-geoengin
2. Lenton T., Rockström J., Gaffney O., Rahmstorf S., Richardson K., Steffen W., Schellnhuber H. (2019) Climate tipping points – Too Risky to bet against, Nature
3. Pattyn F., Ritz C., Hanna E., Asay-Davis X., DeConto R., Durand G., Favier L., Fettweis X., Goelzer H., Golledge N., Munneke P., Lenaerts J., Nowicki S, Payne A., Robinson A., Seroussi H., Trusel L., Broeke M., (2018) The Greenland and Antarctic ice sheets under 1.5 °C global warming, Nature Climate Change
4. Koen G. Helwegen1 , Claudia E. Wieners2,3,a , Jason E. Frank1 , and Henk A. Dijkstra, Complementing CO2 emission reduction by solar radiation management might strongly enhance future welfare, (2019) Earth System Dynamics

5. Latham, J., Rasch, P., Chen, C.-C., Kettles, L., Gadian, A., Gettelman, A., Morrison, H., Bower, K., and Chourlaton, T.: Global temperature stabilization via controlled albedo enhancement of low-level maritime clouds, Philos. T. R. Soc. A, 366, 3969–3987, https://doi.org/10.1098/rsta.2008.0137, 2008.
6. Ahlm, L., Jones, A., Stjern, C. W., Muri, H., Kravitz, B., and Kristjánsson, J. E.: Marine cloud brightening – as effective without clouds, Atmos. Chem. Phys., 17, 13071–13087, https://doi.org/10.5194/acp-17-13071-2017, 2017
7. Gabriel, C. J., Robock, A., Xia, L., Zambri, B., and Kravitz, B.: The G4 Foam Experiment: global climate impacts of regional ocean albedo modification, Atmos. Chem. Phys., 17, 595–613, https://doi.org/10.5194/acp-17-595-2017, 2017
8. Seneviratne, S. I., Phipps, S. J., Pitman, A. J., Hirsch, A. L., Davin, E. L., Donat, M. G., Hirschi, M., Lenton, A., Wilhelm, M., and Kravitz, B.: Land radiative management as contributor to regional-scale climate adaptation and mitigation, Nat. Geosci., 11, 88–96, https://doi.org/10.1038/s41561-017-0057-5, 2018.
9. Cho A, (2016) To fight global warming, Senate calls for study of making Earth reflect more light, Science, https://www.sciencemag.org/news/2016/04/fight-global-warming-senate-calls-study-making-earth-reflect-more-light
10. Levinson, R., Akbari, H. (2010) Potential benefits of cool roofs on commercial buildings: conserving energy, saving money, and reducing emission of greenhouse gases and air pollutants. *Energy Efficiency* 3, 53–109. https://doi.org/10.1007/s12053-008-9038-2
11. Feinberg A., On Geoengineering and Implementing an Albedo Solution with UHI GW and Cooling Estimates vixra 2006.0198, DOI: 10.13140/RG.2.2.26006.37444/6 (Currently in Peer Review in the J. Mitigation and Adaptation Strategies for Global Change)
12. Feinberg A., The Reflectivity (Albedo) Solution Urgently Needed to Stop Climate Change, Youtube, August 2020
13. Paris Climate Accord, (2015) https://unfccc.int/process-and-meetings/the-paris-agreement/what-is-the-paris-agreement
14. Feinberg A. **(**2020) Review of Global Warming Urban Heat Island Forcing Issues Unaddressed by IPCC Suggestions Including CO2 Doubling Estimates, viXra:2001.0415
15. Zhao L., Lee X, Smith R., Oleson K. (2014) Strong, contributions of local background climate to urban heat islands, Nature. 10;511(7508):216-9. doi: 10.1038/nature13462
16. Kiehl, J., Trenberth K. (1997). Earth's annual global mean energy budget. Bulletin of the American Meteorological Society. 78 (2): 197–208:1997, doi:10.1175/1520-0477
17. Myhre, G., Shindell D., Bréon F., Collins W., Fuglestvedt J., Huang J., Koch D., Lamarque J., Lee D., Mendoza B., Nakajima T., Robock A., Stephens G., Takemura T., Zhang H., 2013: Anthropogenic and Natural Radiative Forcing. In: Climate Change 2013: The Physical Science Basis. Contribution of Working Group I to the Fifth Assessment Report of the Intergovernmental Panel on Climate Change, Cambridge University Press
18. Butler J., Montzka S., (2020) The NOAA Annual Greenhouse Gas Index, Earth System Researh Lab. Global Monitoring Laboratory, https://www.esrl.noaa.gov/gmd/aggi/aggi.html
19. McKitrick R. and Michaels J. (2004) A Test of Corrections for Extraneous Signals in Gridded Surface Temperature Data, Climate Research
20. McKitrick R., Michaels P. (2007) Quantifying the influence of anthropogenic surface processes and inhomogeneities on gridded global climate data, J. of Geophysical Research-Atmospheres. Also see McKitrick website describing controversy: https://www.rossmckitrick.com/temperature-data-quality.html
21. Zhao Z. (1991) Temperature change in China for the last 39 years and urban effects. Meteorological Monthly (in Chinese), 17(4), 14-17.
22. Feddema J., Oleson K., Bonan G., Mearns L., Buja L., Meehl G., and Washington W. (2005) The importance of land-cover change in simulating future climates, *Science*, 310, 1674– 1678, doi:10.1126/science.1118160
23. Ren G, Chu Z, Chen Z, Ren Y (2007) Implications of temporal change in urban heat island intensity observed at Beijing and Wuhan stations. *Geophys. Res. Lett.* , *34,* L05711,doi:10.1029/2006GL027927.
24. Ren, G., Chu Z., Zhou J. (2008) Urbanization effects on observed surface air temperature in North China. J. Climate, 21, 1333-1348
25. Jones P., Lister D., and Li Q., (2008) Urbanization effects in large-scale temperature records, with an emphasis on China. J. Geophys. Res., 113, D16122, doi: 10.1029/2008JD009916.

26. Stone B (2009) Land use as climate change mitigation, Environ. Sci. Technol., 43(24), 9052– 9056, doi:10.1021/es902150g
27. Zhao, Z. (2011) Impacts of urbanization on climate change. in: 10,000 Scientific Difficult Problems: Earth Science, 10,000 scientific difficult problems Earth Science Committee Eds., Science Press, 843-846. 30%
28. Yang X, Hou Y, Chen B (2011) Observed surface warming induced by urbanization in east China. *J. Geophys. Res. Atmos*, 116, doi:10.1029/2010JD015452.
29. Huang Q., Lu Y. (2015) Effect of Urban Heat Island on Climate Warming in the Yangtze River Delta Urban Agglomeration in China, *Intern. J. of Environmental Research and Public Health* 12 (8): 8773 (30%)
30. Feinberg A, (2020) Urban Heat Island Amplification Estimates on Global Warming Using an Albedo Model, Vixra 2003.0088, DOI: 10.13140/RG.2.2.32758.14402/15 (Currently under peer review in the journal SN Applied Science)
31. Schmidt G., (2009) Spurious correlations between recent warming and indices of local economic activity, *Int. J. of Climatology*
32. Hartmann, D., Tank A., Rusticucci M., Alexander L., Brönnimann L, Charabi Y., Dentener F., Dlugokencky E., Easterling D., Kaplan A., Soden B., Thorne P., Wild M., Zhai P., 2013: Observations: Atmosphere and Surface. In: Climate Change 2013: The Physical Science Basis. Contribution of Working Group I to the Fifth Assessment Report of the Intergovernmental Panel on Climate Change, Cambridge University Press, Cambridge, United Kingdom and New York, NY, USA.
33. Hanson R. (1991) U.S. Geological Survey, Evapotranspiration and Droughts, https://geochange.er.usgs.gov/sw/changes/natural/et/
34. Paulson, R.W., Chase, E.B., Roberts, R.S., and Moody, D.W., (1988), National Water Summary 1988-89-Hydrologic Events and Floods and Droughts: *U.S. Geological Survey Water-Supply*, 2375, 99-104, https://pubs.er.usgs.gov/publication/wsp2375
35. Cao C, Zhao J., Gong P., Ma G., Bao D, Tian K. (2011) Wetland changes and droughts in southwestern China, *Geomatics, Natural Hazards and Risk*, https://www.tandfonline.com/doi/full/10.1080/19475705.2011.588253
36. Hirshi M., Seneviratne S., Alexandrov V., Boberg F., Boroneant C., Christensen O., Formayer H., Orlowsky B., Stepanek P., (2011) Observational evidence for soil-moisture impact on hot extremes in Europe, *Nature Geoscience* 4, 17-21
37. Kanamori H., Kambatuku J., Kotani A., Asai K., Mizuochi H., Fujioka Y, Iijima M. (2017) Analysing the origin of rain- and subsurface water in seasonal wetlands of north-central, Namibia, , Environ. Res. Lett. **12** 034012
38. Fry H., Reyes-Velarde A., (2019) California wastes most of its rainwater, which simply goes down the drain, *LA. Times,*.
39. Cormack L.,Where does all the stormwater go after the Sydney weather clears? The Sydney Morning Hearald, May 2015. https://www.smh.com.au/environment/where-does-all-the-stormwater-go-after-the-sydney-weather-clears-20150430-1mx4ep,html
40. USGS 1900-2006, Materials in Use in U.S. Interstate Highways, https://pubs.usgs.gov/fs/2006/3127/2006-3127.pdf
41. US Population Growth 1900-2006, u-s-history.com/pages/h980.html1
42. NASA 1900-2006 updated, 2020 https://climate.nasa.gov/vital-signs/global-temperature/
43. Deforestation, Wikipedia, https://en.wikipedia.org/wiki/Deforestation
44. Dessler A., Zhang Z., Yang P., (2008) Water-vapor climate feedback inferred from climate fluctuations, 2003–2008, *Geophysical Research Letters*, https://doi.org/10.1029/2008GL035333
45. Stephens G., O'Brien D., Webster P, Pilewski P, Kato S, Li J, (2015) The albedo of Earth, *Rev. of Geophysics*, https://doi.org/10.1002/2014RG000449
46. Kimoto K., (2006) On the Confusion of Planck Feedback Parameters, Energy & Environment (2009)
47. Zhang X, Friedl MA, Schaaf CB, Strahler AH, and Schneider A (2004) The footprint of urban climates on vegetation phenology. *Geophys. Res. Lett. 31, L12209*
48. Zhou D, Zhao S, Zhang L, Sun G and Liu Y (2015) The footprint of urban heat island effect in China, *Scientific Reports*. 5: 11160
49. Schneider A, Friedl M, and Potere D (2009) A new map of global urban extent from MODIS satellite data. Environmental Research Letters, 4(4), 044003, doi:10.1088/ 1748-9326/4/4/044003

50. Global Rural Urban Mapping Project (GRUMP, 2005) Columbia University Socioeconomic Data and Applications Center, Gridded Population of the World and the Global Rural-Urban Mapping Project (GRUMP).
51. Fan Y, Li Y, Bejan A (2017) Horizontal extent of the urban heat dome flow. *Sci Rep* 7, 11681 https://doi.org/10.1038/s41598-017-09917-4